PLANAR WAVE PROPAGATION IN SHOCK TUBES FOR REPLICATING BLAST INJURY

BRIAN R. BIGLER*, ALLEN W. YU* AND CAMERON R. BASS*

* Injury Biomechanics Laboratory (IBL)
Biomedical Engineering, Duke University
101 Science Drive, Box 90281, 27708 Durham, North Carolina, USA
E-mail: Brian.Bigler@Duke.edu

Key Words: *Shock tube, Blast biomechanics, Arbitrary Lagrangian-Eulerian, LS-DYNA.*

Abstract. To replicate clinically relevant blast trauma, shock tubes are often employed. One key assumption in the use of compressed gas or explosive driven shock tubes is that the shock wave output is planar no matter what the cross section of the shock tube and a fully developed shock wave is impinging on the test subject. The current investigation examines the effect of tube cross sectional shape and tube length on flow evolution and shock development to better understand design constraints and limitations when using shock tubes. Three dimensional arbitrary Lagrangian-Eulerian shock tube models were developed and simulated at physiologically relevant burst pressures of 2.32, 4.65, and 6.97 MPa. Results show that planarity develops in a round cross section after approximately 7 diameter lengths down the driven section of the shock tube for the lowest burst level and after 5 diameters lengths for the highest level. Oscillatory off-axis waves are damped by destructive interference in the axisymmetric round cross section. Such damping did not occur in the square shock tube, which continued to show deviation up to 59.6% from planarity even at ten diameter lengths.

1 INTRODUCTION

Injuries associated with blast are the leading cause of mortality and morbidity in recent military conflicts[1-4]. Trauma can result from the impinging blast wave (primary blast), penetrating projectile and fragment impact (secondary blast), whole-body motion and non-penetrating impact (tertiary blast), and burns and other injuries (quaternary blast) [5]. It is believed that primary blast is a principal cause for mild to moderate traumatic brain injury, but the mechanism of injury is still poorly understood. This emphasizes the need for controlled blast experiments that generate repeatable, simplified loading conditions such that the specimen loading condition is well characterized.

Shock tubes are often used to replicate blast injuries in the laboratory. Driven by either compressed gas or small explosive charges, these experiments typically replicate a free field primary blast injury, i.e. the effect of an impinging shock wave on biologic tissues. One assumption inherent in replication of these test conditions is the assumption of shock wave planarity upon test specimen impingement. The impacting shock is assumed to be a traditional Friedlander wave characterized by a sharp rise in pressure followed by exponential decay and

slight underpressure before returning to ambient (see Figure 1). Since mechanisms of blast injury are still poorly understood, the simplification of blast inputs leads to better characterization and repeatability of injury modes. While a more complex waveform could be applied, knowledge of the complete pressure field would be necessary to fully characterize the stress- and strain-state of impacted tissues and subsequent stress and pressure propagation. Such information would be difficult or impractical to obtain in practice as it would interfere with the blast input on the specimen of interest.

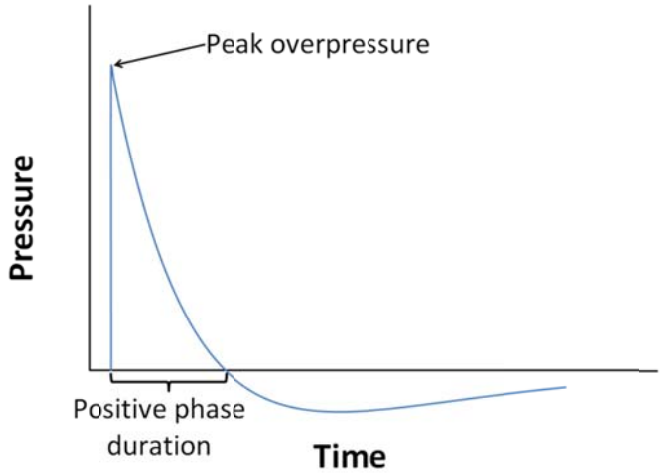

Figure 1. Typical Friedlander free-field blast waveform

Testing with shock tubes is not new. While the focus on traumatic brain injury from blast has increased markedly in recent years, shock tube use has historically been used in aeronautics, gas dynamics, and aerodynamic applications[6]. Simulation of shock tubes has also existed for several decades[7-9]. The classic Sod 1D shock tube problem has become a common benchmark for shock-capturing numeric solvers[6]. Despite their history, these experiments and models are typically performed only in one or two dimensions[10]. While the 2D case may be extended in the case of an axisymmetric round shock tube, such an extension cannot be directly applied to a tube of arbitrary cross section. More recent experiments have examined the effect of driver gas, membrane thickness, driver section length, driven section, length on overpressure and duration output profiles for application to biomechanics of blast[11,12].

Once the capabilities of a designed shock tube are characterized, blast impingement variables such as overpressure and duration can be selected. A confounding factor in replicating blast injury across groups is inconsistency regarding positive phase duration. It has been demonstrated that shock tube testing on animals with masses different from humans must be scaled in order to generate equivalent human exposures. Geometry and mass differences between rodent and small animal models must be scaled to equivalent human exposures[13]. To be relevant to typical improvised explosive device exposure, rodent blast durations scale by a factor of approximately eight[14]. Therefore regardless of cross section, care should be taken to ensure that the designed tube can create blast conditions scalable to high explosives and other clinically relevant human exposures.

2 METHODS

To evaluate the effect of cross-sectional area on flow evolution, two arbitrary Lagrangian-Eulerian (ALE) finite element shock tube models, a square and a round cross section, were constructed. These two cross section shapes represent the vast majority of shock tubes found in current blast literature[15,16]. Artificial bulk viscosity was used to capture shock propagation. Models consisted of a high-pressure driver region, an ambient driven section, and additional ambient volume for expansion at the end of the tube. Models were constructed with matched hydraulic diameters of 76 mm, a one diameter driver section and a ten-diameter driven section. These dimensions were chosen as previous studies have shown them to produce physiologically relevant overpressure and duration, and are of a suitable size for rodent injury models[11]. A mesh density of 1mm was selected as this has previously been shown to be sufficient to capture the response in shock tube simulations [17]. Models were run in quarter-symmetry for efficiency. Mesh statistics are displayed in

Table 1.

Table 1: Mesh statistics for shock tube simulation

Cross section	Round	Square
Hydraulic diameter (mm)	76	76
Driver length (mm)	76	76
Driven length (mm)	760	760
Initial driver volume behind membrane (mm^3)	105,000	134,000
Mesh density (mm)	1	1
Number of elements	1.42E6	3.26E6

The volume behind the membrane was approximated based on deformed geometry of a constrained 2D 0.5 mm membrane with elastic properties (ρ = 1.39E-6 g/mm^3, E = 4895 MPa, ν = 0.4) and applied 2 MPa pressure. Membrane burst was assumed to be instantaneous. Tubes were simulated at three burst levels corresponding to previous round tube experimental tests with 0.5 mm, 1.0 mm, and 1.5 mm membranes[11]. Pressure in the driver section was initialized to 2.32, 4.65, and 6.97 MPa for the three levels, respectively, via a gamma-law equation of state. Initial conditions are defined in Table 2, where E0 is the initial internal energy per unit reference volume, V0 is the initial relative volume, and γ is the ratio of specific heats[18]. Models were constructed using LS-PrePost 4.0 and run in LS-DYNA R7.0.0 (Livermore Software Technologies Corp., Livermore, CA, USA). Subsets of elements were selected within the cross section for each model with a temporal output resolution of 1 μs. The locations of these elements are shown in Figure 2.

Table 2: Gas initial conditions

Driver gas	
E0	1.726, 3.4522, 5.178
V0	0.300
γ	1.404
Ambient gas (driven and expansion)	
E0	0.253
V0	1.000
γ	1.400

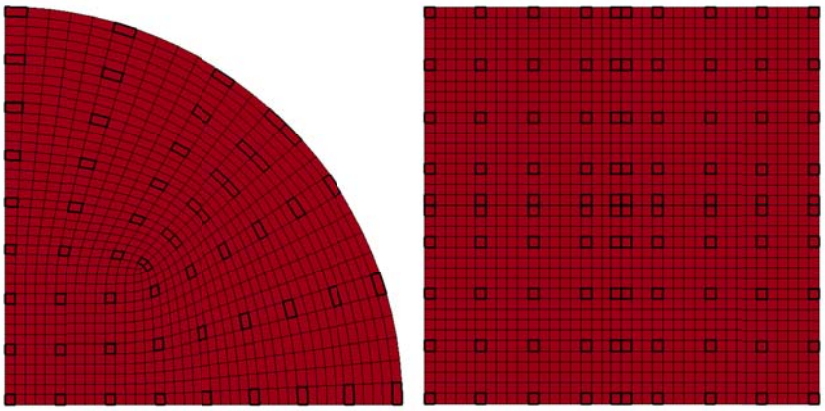

Figure 2. Element locations for pressure output in the round tube (left) and square tube (right) models.

3 Results

Numerical results are presented in Figure 3. The peak pressure at the tube centerline (bottom right corner of inlays, intersection of the two planes of symmetry) for each individual capture plane was used to normalize the pressure field. Moving down the rows, the round tube stabilizes with downstream propagation. This stabilization occurs sooner with increasing shock strength, stabilizing to within 10% after approximately 7, 6, and 5 diameter lengths from lowest to highest burst levelks . Pressure in the capture plane oscillated as the shock front propagated downstream, with off-axis components of the shock front reflecting between the tube boundaries and the centerline. This presented as large volumes of turbulence within the tube and disruption of pressure contours. It can clearly be seen in the 6.97 MPa square tube after 4 and 7 diameter lengths, where pressures correspond to increases 37.2% and 27.3% relative to centerline pressure. While slightly present in the round tube, this effect was more pronounced with the square tube and correlated with increasing burst pressure. Deviation at exit from centerline pressure in the round tube was -1.3%, -5.4%, and -4.4%, respectively, for burst pressures of 2.32, 4.65, and 6.97 MPa. In the square tube, pressure deviation was between -7.3% and -59.6% moving radially toward the tube corner (upper right) for the 2.32 MPa burst, -11.2% at 4.65 MPa burst, and between -13.4% and -31.3% at the highest burst level. The oscillation did decay slightly with time, indicating that convergence to a planar condition might occur beyond the simulated tube.

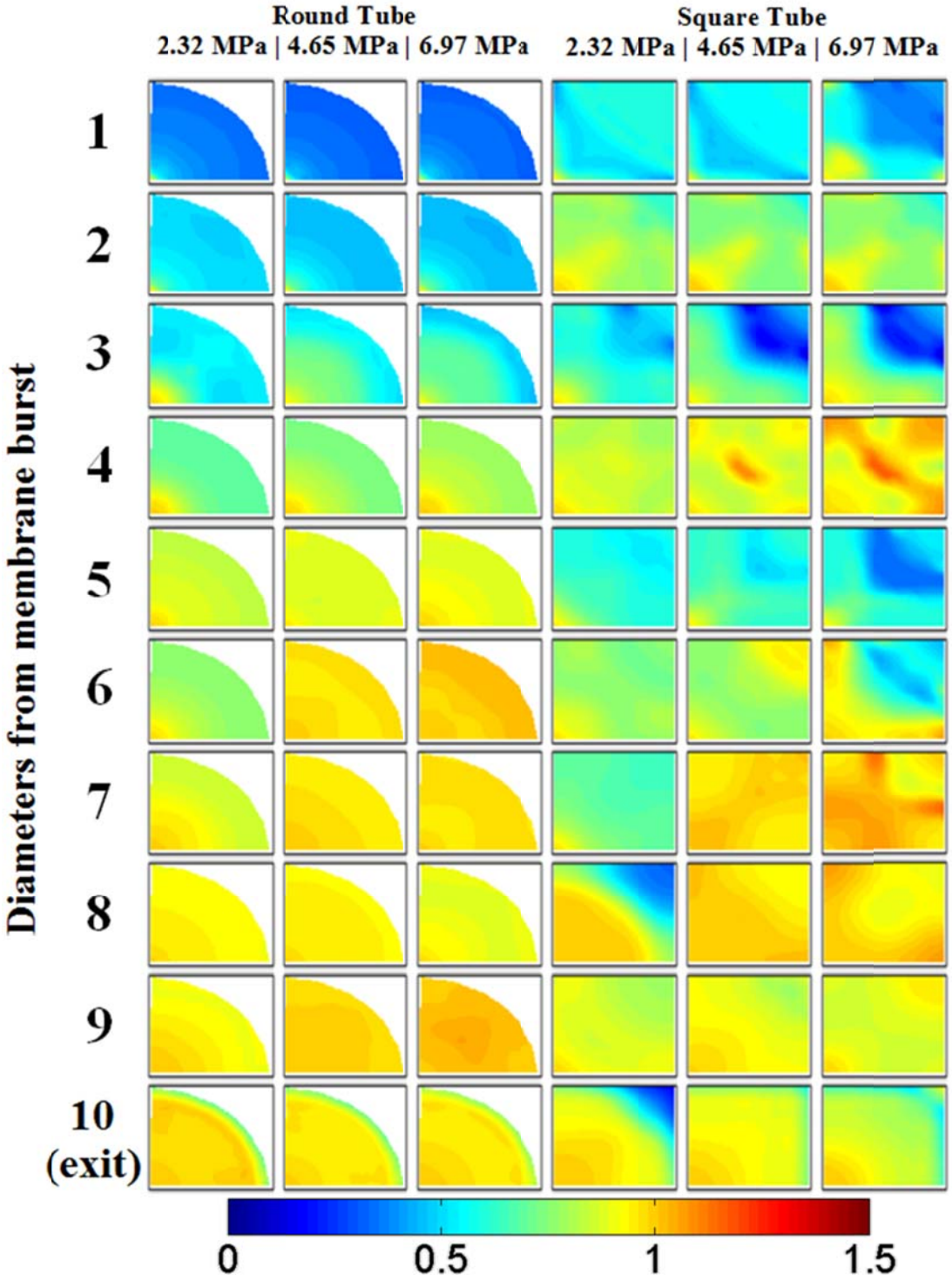

Figure 3. Pressure contours for round and square shock tube simulations for three burst levels. Results normalized to tube centerline peak pressure for each respective figure (bottom left corner of each inlay).

Planarity of the pressure field at tube exit was observed through time in Figure 4. Each trace represents a single element in the exit plane, and the red trace is the tube centerline. It is clear that while the square and round tubes exhibit comparable rise times and peak overpressures, the traces in the round case arrive at the same time, whereas the square tube traces arrive over a period of approximately 2-4 μs and exhibit qualitatively different amplitudes. Both square and round cases exhibit some boundary effects as evidenced by the few separately grouped traces.

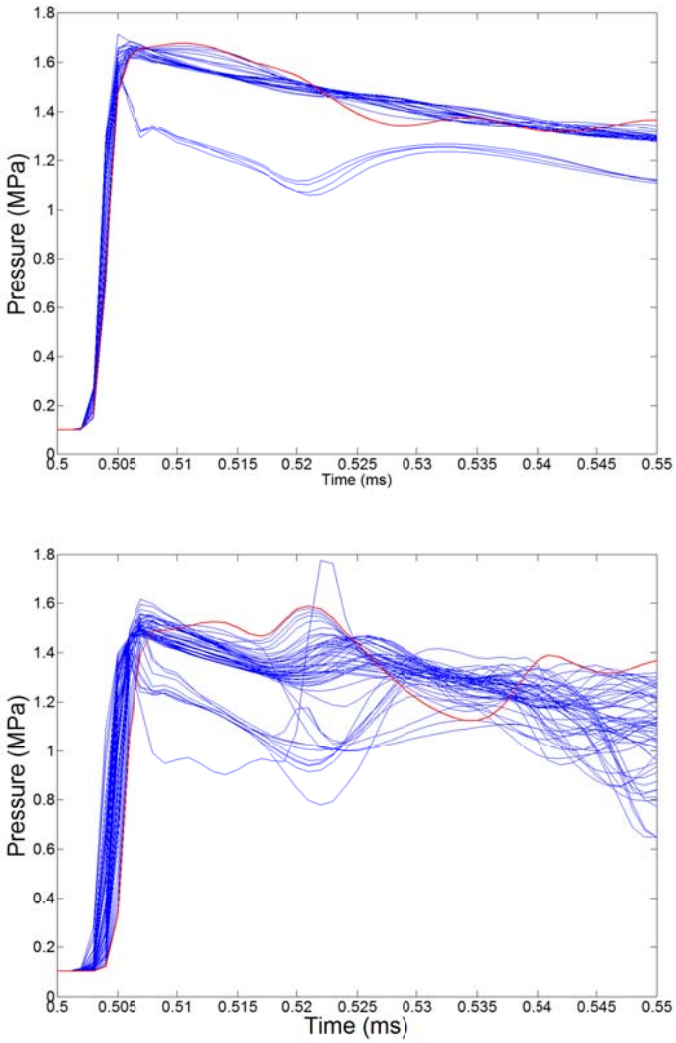

Figure 4. Pressure-time traces for elements in plane of tube exit for 6.97 MPa burst case. Round tube (top) exhibits less variability in the shock front arrival time than the square tube (bottom).

4 CONCLUSIONS

Shock tube simulations demonstrating differences between cross-sectional geometry were conducted. The oscillatory wave propagation between tube boundary and tube centerline causes disruption of wave planarity and impedes reproducible shock output for application to biomechanics of blast. While this effect is present in the round tube, the curvature of the tube wall aids in focusing these reflections and effectively damps spurious off-axis propagation. Due to the sharp corner in the square tube, this focusing is unable to occur, although variance in peak pressure did decline with distance. While the difference in arrival time across the pressure field is small, it serves as a confounding factor when evaluating the effective blast input on any specimen testing. More worrisome is these off-axis waves can constructively or destructively interfere with the axial propagation depending on their phase, creating differences in magnitude across the plane and generating a non-uniform wave front. Furthermore, if a large off-axis component is present in local regions of the incoming shock front, there is the potential for inducing unintended shear loading on the specimen. As a consequence of these findings, the assumption of a simple planar wave impingement is no longer valid for a square shock tube.

As interest in shock tube testing for replicating blast exposure in animal models continues, standardization of testing conditions is critical. We show in this study the advantages of a round shock tube over a square shock tube. Additionally, given the axisymmetric geometry of a round tube and the benefit of generating a planar shock sooner, a shorter driven section may be used which is important in a realistic laboratory setting to generate appropriate blast conditions. The positioning of an animal inside versus outside the tube, both of which are often done in the literature, calls the validity of measured blast exposure into question. Specimen placed inside the shock tube may be within a region that violates the planar shock assumption. Additionally, although beyond the scope of the current study, confinement effects from waves reflecting off the specimen would likely further confuse determination of actual exposure.

REFERENCES

[1.] Bird SM, Fairweather CB. Military fatality rates (by cause) in Afghanistan and Iraq: a measure of hostilities. *International Journal of Epidemiology.* 2007;36(4):841-846.

[2.] Brethauer SA, Chao A, Chambers LW, et al. Invasion vs insurgency: US Navy/Marine corps forward surgical care during Operation Iraqi Freedom. *Archives of Surgery.* 2008;143(6):564-569.

[3.] Capehart B, Bass D. Review: managing posttraumatic stress disorder in combat veterans with comorbid traumatic brain injury. *Journal of Rehabilitation Research & Development.* 2012;49(6).

[4.] Wade AL, Dye JL, Mohrle CR, Galarneau MR. Head, face, and neck injuries during Operation Iraqi Freedom II: results from the US navy-marine corps combat trauma registry. *Journal of Trauma-Injury, Infection, and Critical Care.* 2007;63(4):836-840.

[5.] White CS, Jones RK, Damon EG, Fletcher ER, Richmond DR. *The biodynamics of air blast*: DTIC Document;1971.

[6.] Sod GA. A survey of several finite difference methods for systems of nonlinear hyperbolic conservation laws. *Journal of Computational Physics.* 1978;27(1):1-31.

[7.] Jiang Z, Onodera O, Takayama K. Evolution of shock waves and the primary vortex loop discharged from a square cross-sectional tube. *Shock Waves.* 1999;9(1):1-10.

[8.] Oran E, Young T, Boris J, Cohen A. Weak and strong ignition. I. Numerical simulations of shock tube experiments. *Combustion and Flame.* 1982;48:135-148.

[9.] Chester W. CXLV. The quasi-cylindrical shock tube. *Philosophical Magazine.* 1954;45(371):1293-1301.

[10.] Woodward P, Colella P. The numerical simulation of two-dimensional fluid flow with strong shocks. *Journal of Computational Physics.* 1984;54(1):115-173.

[11.] Panzer MB, Matthews KA, Allen WY, Barclay Morrison III DFM, Bass CR. A multiscale approach to blast neurotrauma modeling: part I–development of novel test devices for in vivo and in vitro blast injury models. *Frontiers in neurology.* 2012;3.

[12.] Sundaramurthy A, Gupta RK, Chandra N. Design Considerations for Compression Gas Driven Shock Tube to Replicate Field Relevant Primary Blast Condition. Paper presented at: ASME 2013 International Mechanical Engineering Congress and Exposition2013.

[13.] Rafaels K, "Dale" Bass CR, Salzar RS, et al. Survival risk assessment for primary blast exposures to the head. *Journal of neurotrauma.* 2011;28(11):2319-2328.

[14.] Wood GW, Panzer MB, Allen WY, Rafaels KA, Matthews KA, Bass CR. Scaling in Blast Neurotrauma. Paper presented at: International Research Council on Biomechanics of Injury2013; Gothenburg, Sweden.

[15.] Ganpule S, Alai A, Plougonven E, Chandra N. Mechanics of blast loading on the head models in the study of traumatic brain injury using experimental and computational approaches. *Biomechanics and modeling in mechanobiology.* 2013;12(3):511-531.

[16.] Shridharani JK, Wood GW, Panzer MB, et al. Porcine head response to blast. *Frontiers in neurology.* 2012;3.

[17.] Panzer MB, Myers BS, Bass CR. Mesh considerations for finite element blast modelling in biomechanics. *Computer methods in biomechanics and biomedical engineering.* 2013;16(6):612-621.

[18.] Hallquist JO. LS-DYNA keyword user's manual. *Livermore Software Technology Corporation.* 2007.